Malaysian Journal of Chemistry, 2024, Vol. 26(1), 16-26
(Special Issue: *International Conference on Natural Products, ICNP 2023*)

Synthesis and Optimization of Azadirachta Excelsa Extract Loaded Chitosan Nanoparticles for Potential Biopesticide Applications

Rohimah Abdun Masaree[1], Nor Hayati Abdullah[2], Tumirah Khadiran[2], Saidatul Husni Saidin[2], Mazura Md. Pisar[2] and Azila Abdul-Aziz[1,3]*

[1]Department of Chemical and Environmental Engineering, Malaysia-Japan International Institute of Technology, Universiti Teknologi Malaysia, Jalan Sultan Yahya Petra, Kuala Lumpur 54100, Malaysia
[2]Forest Research Institute Malaysia, 52109 Kepong, Malaysia
[3]Institute of Bioproduct Development, Universiti Teknologi Malaysia, 71760 Johor Bahru, Johor, Malaysia
*Corresponding author (e-mail: r-azila@utm.my)

Chemical based pesticides are widely used worldwide. However, there are potential health and environmental effects arising from the use of this type of pesticide. To overcome these problems, people are turning to natural approaches to address this issue. *Azadirachta excelsa* (*A. excelsa*) is a plant that can be found in Malaysia and its extract has the potential to be utilized as a biopesticide. However, the shortcomings of the use of biopesticides compared to conventional pesticides include slower rate of control, lower efficacy, shorter persistence, and greater susceptibility to changes in environmental conditions. To address some of these issues, *A. excelsa* extract was encapsulated in chitosan nanoparticles. The encapsulation of *A. excelsa* extract into chitosan nanoparticles was optimized using Central Composite Design (CCD) of Response Surface Methodology. The independent variables selected include chitosan's concentration, chitosan:Tripolyphosphate (TPP) ratio and time of sonication; and the responses studied include size, Polydispersity Index (PDI), zeta potential, encapsulation efficiency and drug loading. The responses were predicted using second order polynomial model. The optimum condition for the preparation of *A. excelsa* extract loaded chitosan nanoparticles was 1.0 mg/mL of chitosan's concentration, chitosan:TPP ratio of 4:1 and time of sonication of 3 minutes. The size, PDI, zeta potential, encapsulation efficiency and drug loading at optimum condition were 201.8 nm, 0.390, 86.6 mV, 89.8% and 4.9%, respectively. Transmission electron microscopy (TEM) images of chitosan nanoparticles revealed particles with smooth spherical shape. The study showed that interaction among chitosan's concentration, chitosan:TPP ratio and time of sonication can significantly change the physical characteristics of chitosan nanoparticles, and this provide an avenue for the formulators to engineer chitosan nanoparticles according to needs.

Keywords: Chitosan nanoparticles; optimization; *Azadirachta excelsa*

Received: September 2023; Accepted: November 2023

Azadirachta excelsa is a plant found in lowland dipterocarp forests up to 350 m in altitude in south-east Asia. It typically grows in ancient clearings or secondary forest [1]. The plant has an early development period which is often free of pest and disease issues. Its growth is slow initially but subsequently increases significantly [2]. *Azadirachta excelsa*, which is related to Indian neem (*Azadirachta indica* [3]), has been used as a pesticide in a few studies. It is expected that *Azadirachta excelsa* will have similar biopesticide potential with *Azadirachta indica*. The colloquial name for *Azadirachta indica* is neem. It is sometimes referred to as margosa and is a member of the Meliaceae family.

According to [4], these plants are found to be abundant in limonoids. Thus far, several insecticidal active components have been identified in plants belonging to the Meliaceae family. Triterpenoids are primarily responsible for the high insecticidal power of the Meliaceae plants [5, 6]. Numerous of these triterpenoids have demonstrated antifeedant, stomach poison, contact poison, and growth inhibition properties on several significant agricultural insects. It is suggested that neem's non-wood components, such as its bark, leaves, fruits, flowers, gum, oil, and neem cake, contain biological properties that include larvicidal, nematicidal, antifeedant, and insecticidal effects [5]. Azadirachtin (Figure 1), a triterpenoid that is known to stop insect metamorphosis, is the main active component of neem. This ingredient mostly affects termites, aphids, and weevils. A large number of neem biopesticides have reached the market [6]. However, the shortcomings of the use of bio-pesticides compared to conventional pesticides include slower rate of control, lower efficacy,

†Paper presented at the International Conference on Natural Products 2023 (ICNP 2023)

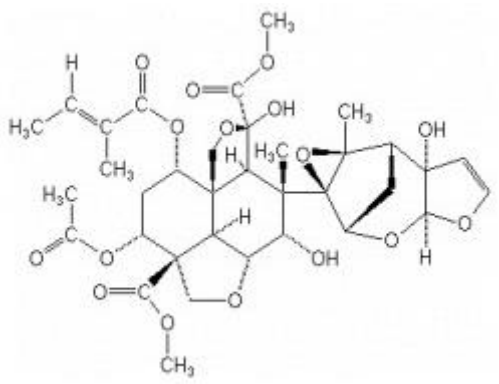

Azadirachtin

Figure 1: Structure of Azadirachtin.

shorter persistence and greater susceptibility to changes in environmental conditions.

In agriculture, chitosan nanoparticles can function as growth enhancers and strong antibacterial agents against harmful fungus and bacteria [7]. In addition, chitosan can also act as nanocarriers for agrochemicals [8, 9, 10]. To develop an efficient nano delivery system formulation, the agriculturally active chemical can be encapsulated using ionic or covalent inter/intramolecular bonds or trapped in a polymeric matrix of chitosan [10]. The ionic gelation method is often used to create chitosan nanoparticulate systems due to its simplicity and low cost. The technique uses fewer chemicals than other methods, which minimizes any potential hazardous side effects. It uses acidic polyanions with a negative charge, such as tripolyphosphate (TPP), to form a link with chitosan's positively charged protonated amino group [11].

In this study, Response Surface Methodology (RSM) was utilized to optimize the process of encapsulating *Azadirachta excelsa* extract in chitosan using ionic gelation method. The parameters studied were chitosan's concentration, chitosan: TPP ratio and time of sonication. RSM is a statistical model which develops the best factor and level settings for optimizing process parameters using randomized and minimal experimental runs. Central composite design (CCD) of the RSM provides data for multivariable system modelling and was utilized in this research work for interpreting the individual and interactional effect of chitosan's concentration, chitosan: TPP ratio and time of sonication on the encapsulation process.

EXPERIMENTAL

Chemicals and Materials

Chitosan, tripolyphosphate (TPP) and *acetic acid* were obtained from R&M Chemicals, India. *Ethanol*

was obtained from Systerm, Malaysia. Ursolic acid (Sigma Aldrich, USA), vanillin (Ajax Chemicals, Australia), acetic acid (R & M Chemicals, India), perchloric acid (Systerm, Malaysia) and *ethyl acetate* (EMSURE, Germany) were also used in this study. All chemicals were used as received unless otherwise stated.

Characterization Methods

Experimental Design

The optimization of the encapsulation process of *A. excelsa* extract chitosan nanoparticles was performed based on RSM via Design Expert® software (Version 13, StatEase, Minneapolis, USA). Three independent variables and respective values were selected for the optimization process which were chitosan's concentration, A (0.5, 1.0, 2.0, 2.5, 3.0 mg/mL), chitosan: TPP ratio, B (3:1, 4:1, 5.5:1, 7:1, 8:1 mg/mL), and time of sonication, C (2, 3, 4, 5, 6 min) [12]. Experimental design consisted of 20 randomized runs which included eight factorial points, eight axial points and four unknown points including the replicates. The responses of the study were the size, polydispersity index (PDI), zeta potential, encapsulation efficiency and drug loading of nanoparticles.

Encapsulation of *A. excelsa* in Chitosan Nanoparticles using Ionic Gelation Method

An appropriate amount of chitosan was dissolved in 1.0% acetic acid using a magnetic stirrer (at 50°C for 2-5 hours). An appropriate amount of TPP was dissolved in deionized water. 1.0 g/ml of *A. excelsa ethanolic* extract was added to the TPP solution with a ratio of 2:1 (TPP:Extract). Then, the TPP mixture was added dropwise into the chitosan mixture whilst stirring for 1 hour. Next, the chitosan mixture was sonicated using a probe sonicator. The preparation of the chitosan nanoparticles was based on the method described by Hoang et. al. [13]

Size and Zeta Potential Characterization

The nanoparticles were characterized via Dynamic Light Scattering (DLS) using Malvern Zetasizer Nano S equipment (Malvern Instruments, Worcestershire, UK) for size, PDI and zeta potential. The samples were diluted with deionized water (1:5 and 1:10) before conducting the analysis [14].

Encapsulation Efficiency and Drug Loading using Calorimetric Method

1 mL samples were centrifuged at 12000 rpm for 30 minutes. The supernatant layer was carefully removed and mixed with *methanol*. Uncentrifuged samples were sonicated for 30 minutes. For both the centrifuged and uncentrifuged samples, 0.2 mL samples were placed in calorimetric tubes, 0.2 mL of 5% vanillin-acetic acid and 1.2 mL perchloric acid were then added. The vials of solution were incubated in a 70°C water bath for 15 minutes. Afterwards the vials were rinsed in running water for 2 minutes. *Ethyl acetate* was added until the volume was 5 mL and then cooled to room temperature. The samples were measured using a spectrophotometer at 550 nm. The encapsulation efficiency and drug loading were then calculated using equations (1) and (2), respectively [15].

Morphology Analysis using Transmission Electron Microscopy (TEM)

Morphology analysis was conducted using TEM (Jeol-1200 EX II-TEM, Columbia, MD, USA). Nanoparticle dispersions were diluted at a ratio of 1:100 with ultrapure Milli-Q® water, and 10 µl of the resulting mixture was applied to a 400-mesh copper grid. A paper filter was used after incubation to eliminate extra sample. For contrast enhancement, one drop of phosphotungstic acid was applied to the grid. The grid was then incubated at 25°C for one minute before any excess was removed. The grid was finally dried at ambient temperature [16].

Fourier Transform Infrared (FTIR) Spectroscopy Analysis

A Nicolet 6700 spectrometer from Thermo Scientific, Inc. in Waltham, Massachusetts, USA, was used to obtain FTIR spectra. The attenuated total reflectance (ATR) mode was utilized to record spectra with a resolution of 2 cm^{-1} spanning the range of 450 – 4000 cm^{-1} [16].

RESULTS AND DISCUSSION

Analysis of Response Surface Models

Full factorial design of CCD was applied to evaluate the effect of the parameters on response values and to identify optimized conditions for nanoparticle formulation. Second order polynomial quadratic model in terms of actual factors was developed to estimate the response value by carrying out multiple regression analysis (Eq 3), (Eq 4), (Eq 5), (Eq 6) and (Eq 7) where actual values of extraction parameters are represented as A, B and C.

$$\text{Encapsulation efficiency (\%)} = \frac{\text{Initial amount of } A.\ excelsa \text{ extract} - \text{Free } A.\ excelsa \text{ extract}}{\text{Initial amount of } A.\ excelsa} \times 100\ \% \quad (1)$$

$$\text{Drug Loading (\%)} = \frac{\text{Initial amount of } A.\ excelsa \text{ extract} - \text{Free } A.\ excelsa \text{ extract}}{\text{Mass of carrier}} \times 100\ \% \quad (2)$$

$$\text{Size} = 405.11215 + 155.16003\ A - 88.42449\ B - 56.82626\ C - 11.19245\ AB - 30.73684\ AC + 6.38333\ BC + 20.66604\ A^2 + 7.34651\ B^2 + 9.55306\ C^2 \quad (3)$$

$$\text{PDI} = 1.15732 - 0.178461\ A - 0.178899\ B - 0.089309\ C + 0.018862\ AB - 0.024053\ AC - 0.001667\ BC + 0.036534\ A^2 + 0.014121\ B^2 + 0.016119\ C^2 \quad (4)$$

$$\text{Zeta Potential} = -5.55782 + 33.38908\ A - 2.4113\ B + 38.52486\ C - 0.148664\ AB - 5.23158\ AC - 1.4\ BC - 3.91024\ A^2 + 0.670027\ B^2 - 2.54883\ C^2 \quad (5)$$

$$\text{Encapsulation Efficiency} = 144.13919 - 44.80447\ A - 6.2949\ B - 1.42177\ C + 1.62098\ AB + 4.27211\ AC + 0.0181667\ BC + 3.95244\ A^2 + 0.223520\ B^2 - 1.08829\ C^2 \quad (6)$$

$$\text{Drug Loading} = 1.81451 + 0.438140\ A - 0.406275\ B + 2.04287\ C + 0.027108\ AB - 1.00342\ AC + 0.200833\ BC + 0.394926\ A^2 - 0.060319\ B^2 - 0.101770\ C^2 \quad (7)$$

Table 1. Experimental value of ANOVA for the response surface quadratic model.

Source	Size (nm) (R^2= 0.9497)					PDI (R^2= 0.9769)					Zeta potential (mV) (R^2= 0.9414)				
	SS	df	MS	F-value	p-value	SS	df	MS	F-value	p-value	SS	df	MS	F-value	p-value
Model	25668.33	9	2852.04	20.99	< 0.0001	0.0493	9	0.0055	46.99	< 0.0001	488.10	9	54.23	17.84	< 0.0001
A: Chitosan's concentration	14274.20	1	14274.20	105.04	< 0.0001	0.0143	1	0.0143	122.92	< 0.0001	32.17	1	32.17	10.58	0.0087
B: Chitosan: TPP ratio	82.20	1	82.20	0.6049	0.4547	0.0002	1	0.0002	1.95	0.1926	24.04	1	24.04	7.91	0.0184
C: Time of sonication	12.78	1	12.78	0.0941	0.7653	0.0021	1	0.0021	17.60	0.0018	24.86	1	24.86	8.18	0.0170
AB	1326.13	1	1326.13	9.76	0.0108	0.0038	1	0.0038	32.31	0.0002	0.2340	1	0.2340	0.0770	0.7871
AC	4487.58	1	4487.58	33.02	0.0002	0.0027	1	0.0027	23.58	0.0007	130.00	1	130.00	42.76	< 0.0001
BC	733.44	1	733.44	5.40	0.0425	0.0001	1	0.0001	0.4290	0.5273	35.28	1	35.28	11.60	0.0067
A^2	1620.91	1	1620.91	11.93	0.0062	0.0051	1	0.0051	43.46	< 0.0001	58.03	1	58.03	19.09	0.0014
B^2	3744.23	1	3744.23	27.55	0.0004	0.0138	1	0.0138	118.68	< 0.0001	31.14	1	31.14	10.24	0.0095
C^2	2358.51	1	2358.51	17.36	0.0019	0.0067	1	0.0067	57.61	< 0.0001	167.89	1	167.89	55.22	< 0.0001
Residual	1358.90	10	135.89			0.0012	10	0.0001			30.40	10	3.04		
Lack of Fit	981.87	5	196.37	2.60	0.1585	0.0008	5	0.0002	2.58	0.1605	23.79	5	4.76	3.60	0.0932
Pure Error	377.03	5	75.41			0.0003	5	0.0001			6.61	5	1.32		
Cor Total	27027.23	19				0.0505	19				518.51	19			

Table 2. Experimental value of ANOVA for the response surface quadratic model.

Source	Encapsulation efficiency (%) (R^2= 0.9341)					Drug loading (%) (R^2= 0.9895)				
	SS	df	MS	F-value	p-value	SS	df	MS	F-value	p-value
Model	480.20	9	53.36	15.74	< 0.0001	45.93	9	5.10	104.69	< 0.0001
A: Chitosan's concentration	190.60	1	190.60	56.23	< 0.0001	32.28	1	32.28	662.26	< 0.0001
B: Chitosan: TPP ratio	2.20	1	2.20	0.6500	0.4389	1.42	1	1.42	29.13	0.0003
C: Time of sonication	41.52	1	41.52	12.25	0.0057	5.07	1	5.07	103.92	< 0.0001
AB	27.82	1	27.82	8.21	0.0168	0.0078	1	0.0078	0.1596	0.6979
AC	86.69	1	86.69	25.58	0.0005	4.78	1	4.78	98.11	< 0.0001
BC	0.5941	1	0.5941	0.1753	0.6843	0.7260	1	0.7260	14.89	0.0032
A^2	59.29	1	59.29	17.49	0.0019	0.5919	1	0.5919	12.14	0.0059
B^2	3.47	1	3.47	1.02	0.3357	0.2524	1	0.2524	5.18	0.0461
C^2	30.61	1	30.61	9.03	0.0132	0.2677	1	0.2677	5.49	0.0411
Residual	33.89	10	3.39			0.4875	10	0.0487		
Lack of Fit	24.56	5	4.91	2.63	0.1559	0.3941	5	0.0788	4.22	0.0700
Pure Error	9.33	5	1.87			0.0933	5	0.0187		
Cor Total	514.10	19				46.41	19			

The best fitted quadratic model for the three parameters was obtained via ANOVA analysis (Table 1 and 2). The coefficient of determination, R^2 values of size, PDI, zeta potential, encapsulation efficiency and drug loading were 0.9497, 0.9769, 0.9414, 0.9341 and 0.9895, respectively which were not very close to unity but were still viable due to the high significance of the developed models ($p < 0.0001$). R^2 value larger than 80% indicated adequate agreement among actual and predicted values which proves the developed models are statistically sound and can be used to study the effects of parameters on response values [17]. For the Lack of fit analysis, replicated design points residual error was compared to pure error, indicating the differences among responses around the fitted model. ANOVA analysis revealed that chitosan's

concentration had the most significant influence on size, PDI, zeta potential, encapsulation efficiency and drug loading as the F-value of chitosan's concentration for all responses are the highest compared to chitosan: TPP ratio and time of sonication. Further interpretation of RSM surface plots were carried out to understand the interaction effects of chitosan's concentration with other parameters on response.

Effects of Independent Variables on Size, PDI, Zeta Potential, Encapsulation Efficiency and Drug Loading

Figures 2, 3, 4, 5 and 6 illustrate three-dimensional response surfaces plots by presenting the response of two factors and keeping the other one constant at its middle level. Each figure reveals the effects of the selected parameters on *A. excelsa*-Chitosan nanoparticles. For size, Figure 2a shows more influence on the size of nanoparticles as the shape is more curved than Figure 2b and 2c. Figure 2a shows that the effect of chitosan's concentration (mg/mL) and Chitosan: TPP ratios on the size of nanoparticles at constant time of sonication (mins) appears as a curved shape. The plot shows that as chitosan's concentration and Chitosan: TPP ratio increases, the size of nanoparticles increases. Chitosan concentration significantly affects the size of nanoparticles ($p<0.001$, Table 1). For PDI, Figure 3b shows that low chitosan concentration (mg/mL) and longer time of sonication (min) result in a decrease in PDI values. A low PDI value signifies higher homogeneity in size. Meanwhile, at constant time, the value of PDI slightly decreases as the chitosan concentration and chitosan: TPP ratio increase (Figure 3a). At constant chitosan concentration, PDI slightly increases as the chitosan: TPP ratio and time increase (Figure 3c). Chitosan concentration (mg/mL) significantly affects PDI ($p<0.001$, Table 1).

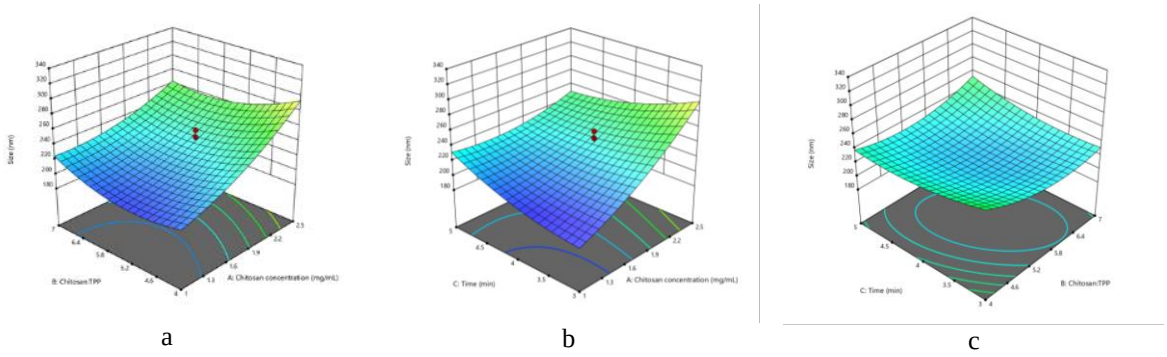

a b c

Figure 2. Response surface plots on size (a) Chitosan's concentration vs Chitosan:TPP ratio, (b) Chitosan's concentration vs Time of sonication, and (c) Chitosan:TPP ratio vs Time of sonication.

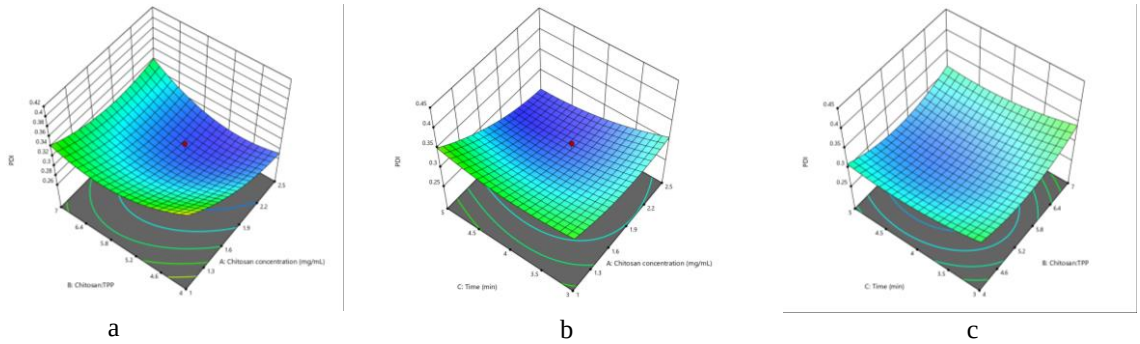

a b c

Figure 3. Response surface plots on PDI (a) Chitosan's concentration vs Chitosan:TPP ratio, (b) Chitosan's concentration vs Time of sonication, and (c) Chitosan:TPP ratio vs Time of sonication.

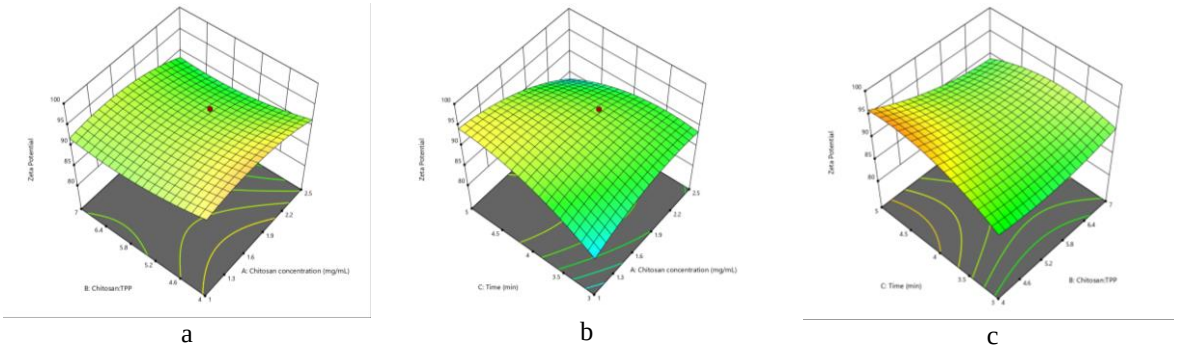

a b c

Figure 4. Response surface plots on zeta potential (a) Chitosan's concentration vs Chitosan:TPP ratio, (b) Chitosan's concentration vs Time of sonication, and (c) Chitosan:TPP ratio vs Time of sonication.

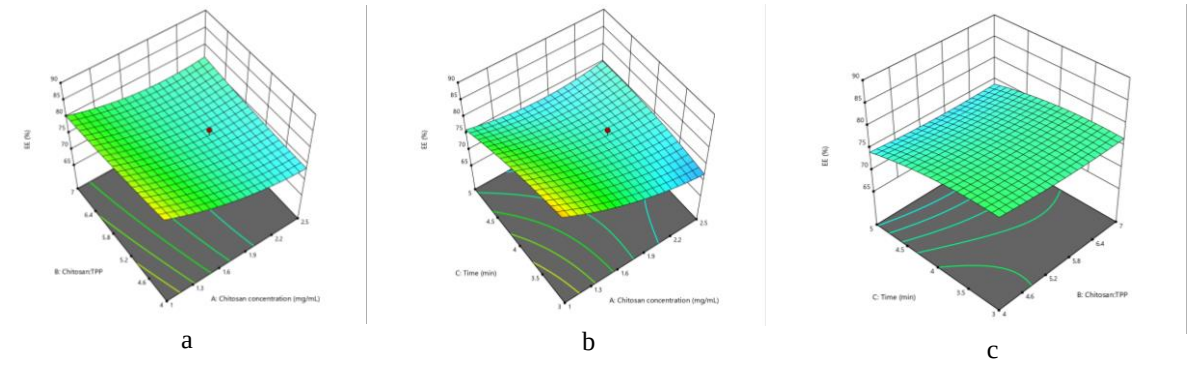

a b c

Figure 5. Response surface plots on encapsulation efficiency (a) Chitosan's concentration vs Chitosan:TPP ratio, (b) Chitosan's concentration vs Time of sonication, and (c) Chitosan:TPP ratio vs Time of sonication.

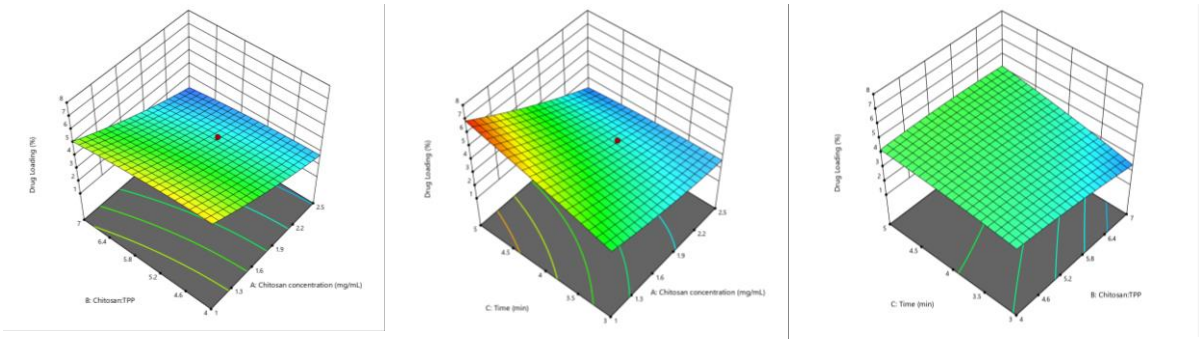

a b c

Figure 6. Response surface plots on drug loading (a) Chitosan's concentration vs Chitosan:TPP ratio, (b) Chitosan's concentration vs Time of sonication, and (c) Chitosan:TPP ratio vs Time of sonication.

As for the zeta potential, the response surface showing the effect of chitosan's concentration and time of sonication on nanoparticles at constant Chitosan: TPP ratio shows decreasing trend (Figure 4b). It shows that the value of the zeta potential gradually decreases with the increase in chitosan's concentration and time of sonication. This indicates that to get higher value of zeta potential, the chitosan's concentration and time of sonication have to be lowered. Next, encapsulation efficiency (EE) shows that at a constant time, as chitosan's concentration increases and chitosan;TPP ratio decreases, the value of EE decreases (Figure 5a). At a constant chitosan: TPP ratio, the value of EE decreases as the chitosan concentration and time increase (Figure 5b). Figure 5c shows that at constant chitosan concentration, as chitosan: TPP ratio and time increase, the response surface is almost horizontal and shows very little

change. Figure 6b shows that as chitosan's concentration and time increase, drug loading decreases. Both chitosan concentration and time of sonication show statistically highly significant effects on drug loading ($p<0.001$, Table 2). Figure 6a shows that as chitosan's concentration and chitosan: TPP ratio increase, the value of drug loading decreases while Figure 6c shows that a minimal change in drug loading value is observed when chitosan's concentration and time of sonication increase.

Characterization

Fourier Transform Infrared (FTIR) Spectroscopy

The chemical structure of chitosan and TPP are shown in Figure 7. FTIR spectra of Chitosan (CS), *A. excelsa ethanolic* extract, Chitosan nanoparticles (CSNPs) and *A. excelsa*-loaded CSNPs are shown in Figure 8, which reveals the occurrence of multiple functional groups in their structure. CS powder (Figure 8b) showed characteristic peaks at 3363.7 (for stretching vibration of OH and NH_2), 2882.2 (C–H bond vibrations in alkanes), 1659.6 (C=O bond vibrations in the amide I molecules), 1378.7 (general OH groups bending), 1155.1 and 1080.9 (correspond to the stretching vibrations of C–O–C bonds), and 607 cm^{-1} (correspond to the vibration of pyranoside rings), which are also confirmed by [15]. It is expected that cross-linking of CS polymer with TPP molecules would shift the peaks related to amide groups. Thus, comparing FTIR spectra of *A. excelsa*-CSNPs, chitosan and empty CSNPs in Figure 8a, b and d reveals that the peak at 3363.7 cm^{-1} ($–NH_2$ groups stretching vibration in CS) was shifted to 3175 cm^{-1} in *A. excelsa*-CSNPs attributing to the occurrence of TPP molecules [18].

In addition, the peaks at 1659.6 and 1421.2 cm^{-1} in CS (relating to C=O stretching of the amide I) were shifted to 1650.4 and 1411.5 cm^{-1} in CSNPs, indicating that the amine groups of CS and poly-anionic phosphate groups of TPP may take part in the reaction [18]. As can be seen in Figure 8c, absorption bands of *A. excelsa ethanolic* extract functional groups are observed. The intense bands occurring at 3339.4 cm^{-1}, 2976.9 cm^{-1}, 2900.9 cm^{-1}, 1658.5 cm^{-1}, 1380.8 cm^{-1}, 1088.9 cm^{-1}, and 878.01 cm^{-1} corresponding to O-H / C-O str/ N-H / O-H str/ C-H/ C=O stretching , bending, vibrations respectively indicate the presence of alcohol, phenol, amines, amides, carboxylic group, ester, ether and amino acids group in leaves of *Azadirachta excelsa* while the peak of 1047.6 cm^{-1} corresponding to the C-O stretching of primary alcohol (*ethanol*) [19].

FTIR analysis was performed to determine if the entrapment of *A. excelsa* within CSNPs is chemical or physical. One could anticipate a physical entrapment if no or very slight changes in the FTIR spectrum were noticed compared to the parental compounds, however one explanation for the spectrum change is a potential chemical reaction between *A. excelsa* and CSNPs. Comparing the FTIR spectra of unloaded and loaded with *A.excelsa*-CSNPs revealed no spectral differences, indicating that *A. excelsa* was physically entrapped (encapsulated) within CSNPs (Figures 8a and 8b). Furthermore, the addition of *A. excelsa* to CSNPs significantly increased the strength of the C-H stretching bands at the locations of 3175, 2882.2, 1411.5, 1421.2, and 1080.9 cm^{-1}, demonstrating the successful encapsulation of *A. excelsa* into CSNPs. Our findings were consistent with those found in past research [15, 20].

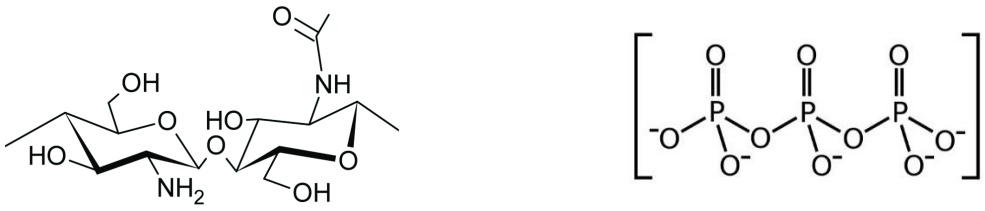

a b

Figure 7. Chemical structure of (a) Chitosan and (b) Tripolyphosphate.

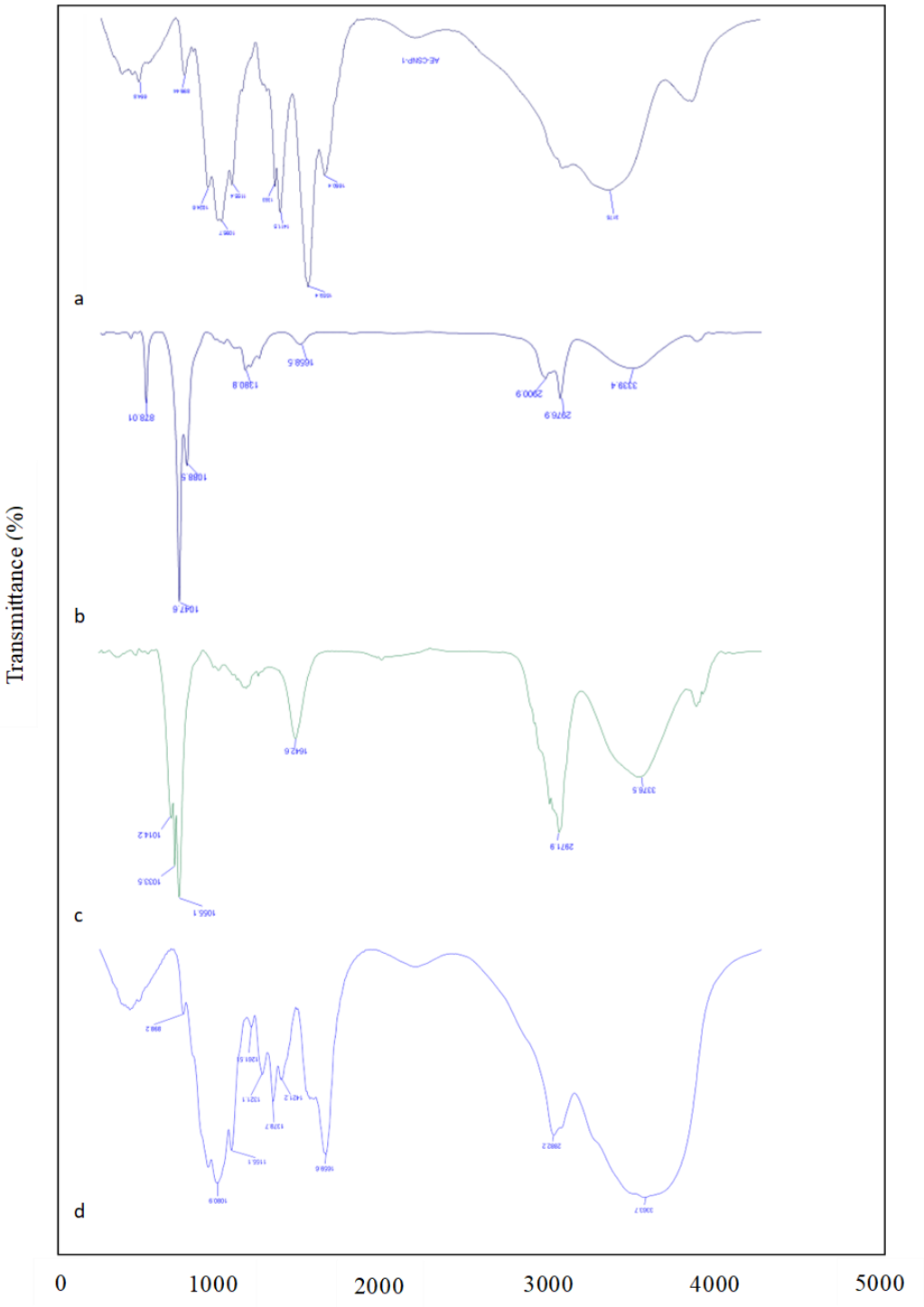

Figure 8. FT-IR spectra of (a) *A. excelsa*-CSNPs, (b) chitosan, (c) *A. excelsa* extract and (d) empty CSNPs.

Morphology Analysis using Transmission Electron Microscopy (TEM)

A. excelsa-CSNPs was successfully prepared using the ionic gelation method. Size, polydispersity index and zeta potential of the nanoparticles were analysed using Dynamic Light Scattering (DLS). The *A. excelsa*-CSNPs optimized value showed the particles' size was 100-200 nm with polydispersity index of 0.390 in ultrapure water and zeta potential of 86.8 mV. TEM images of *A. excelsa*-CSNPs showed smooth spherical nanoparticles (as shown in Figure 9).

CONCLUSION

The study showed that chitosan's concentration was the parameter with the most significant effect on size, PDI, zeta potential, encapsulation efficiency and drug

loading. The optimized condition established by RSM were as follows: 1.0 mg/mL of chitosan's concentration, chitosan: TPP ratio of 4:1 and 3 minutes of time of sonication which led to the formation of *A. excelsa* loaded chitosan nanoparticles with the size of 100-200 nm, PDI of 0.39, zeta potential of 86.6 mV, encapsulation efficiency of 89.9% and drug loading of 4.85%. FTIR results indicated no spectral change between the components of *A. excelsa*-CSNPs, confirming physical entrapment or encapsulation of *A. excelsa* within CSNPs. Overall, CSNPs provide an effective nanomaterial to encapsulate *A. excelsa* extract.

ACKNOWLEDGEMENTS

The authors would like to acknowledge the lab facilities and funding from Grant FRGS/1/2020/STG04/KATS//1 KPTM and PY/2021/02604 R.K130000.7843.5F516 Universiti Teknologi Malaysia. The authors would like to also acknowledge Kahviyaah Letchumanan, Salbiah binti Man, and other lab officers who have greatly assisted the authors in this research.

a.

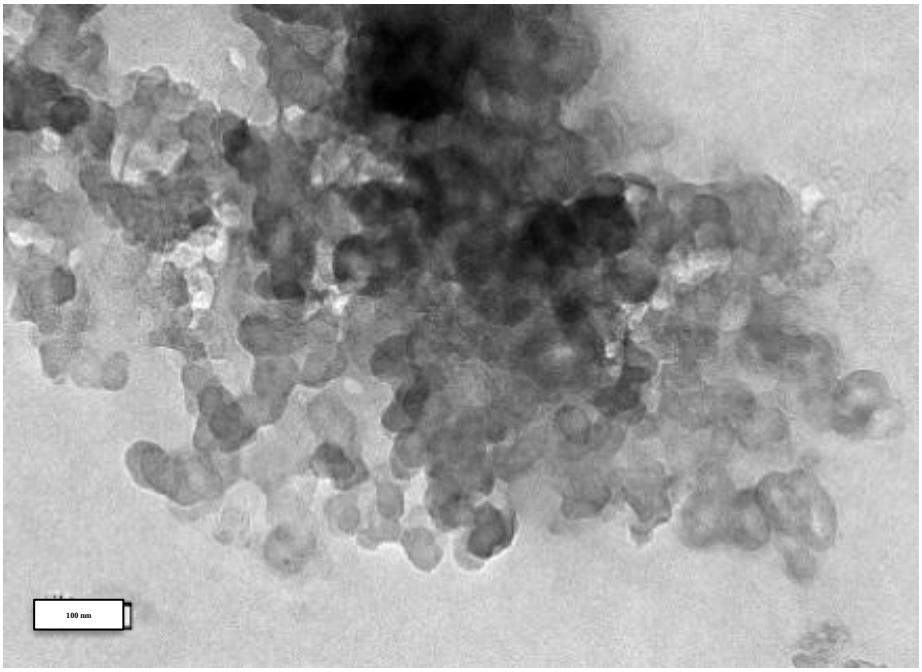

b.

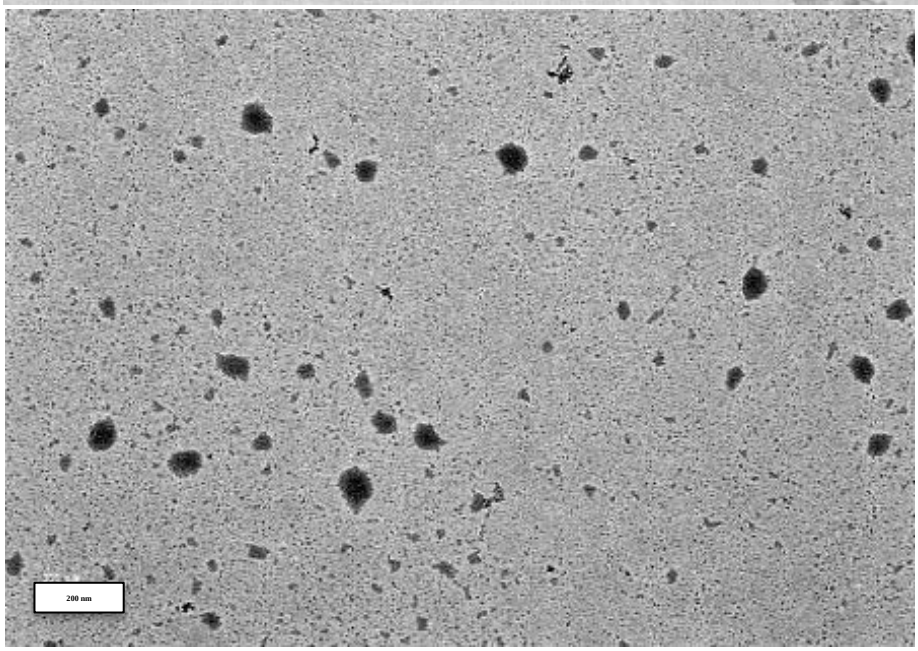

c. 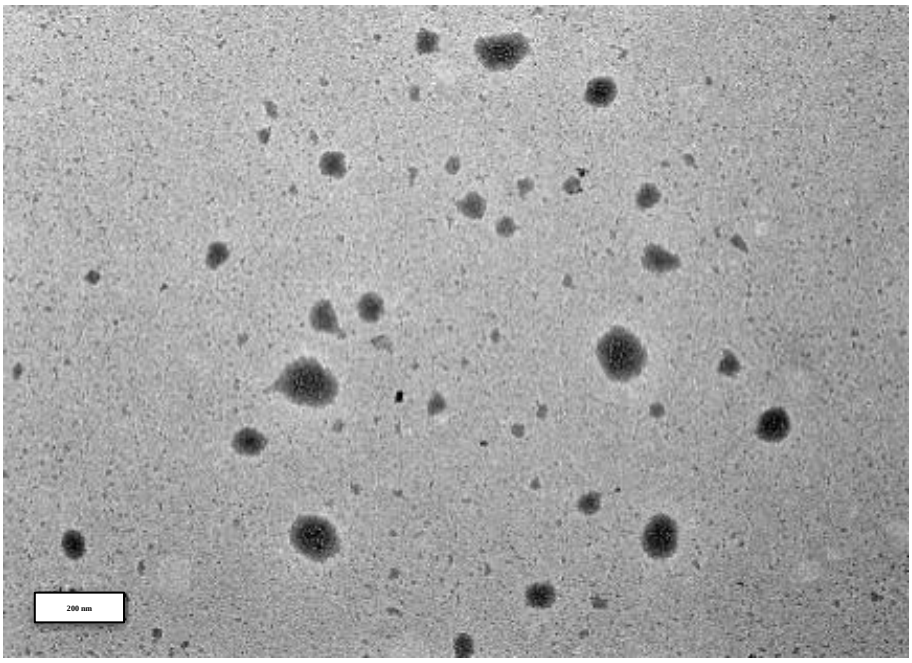

Figure 9. TEM images of (a) Chitosan nanoparticles, CSNPs, (b) Chitosan-TPP nanoparticles and (c) A. excelsa loaded Chitosan-TPP nanoparticles (Chitosan: 1.0 mg/mL; A. excelsa ethanolic extract: 1.0 mg/mL).

REFERENCES

1. Morina Adfa, Khafit Wiradimafan, Ricky Febri Pratama, Angga Sanjaya, Deni Agus Triawan, Salprima Yudha, S., Masayuki Ninomiya, Mohamad Rafi, Mamoru Koketsu (2023) Anti-Termite Activity of Azadirachta excelsa Seed Kernel and Its Isolated Compound against Coptotermes curvignathus. *J. Korean Wood Sci. Technol.*, **51(3)**, 157–172.

2. Orwa, C., Mutua, A., Kindt, R., Jamnadass, R., Anthony, S. (2009) Agroforestree Database: A tree reference and selection guide version 4.0 (http://www.worldagroforestry.org/sites/treedbs/treedatabases.asp)

3. Vaishali Shukla and Md. Rizwan (2015) Green-synthesis and characterization of Silver Nano-particles from Leaves extracts of Azadirachta indica (Neem). *Centre for Nanoscience, Central University of Gujarat, Gandhinagar* – 382030.

4. Lin, M., Yang, S., Huang, J., Zhou, L. (2021) Insecticidal Triterpenes in Meliaceae: Plant Species, Molecules and Activities: Part I (Aphanamixis-Chukrasia). *International Journal of Molecular Sciences*, **22(24)**, 13262. https://doi.org/10.3390/ijms222413262.

5. Kandar, P. (2021) Phytochemicals and bio-pesticides: Development, current challenges and effects on human health and diseases. *J. Biomed. Res.*, **2(1)**, 3–15.

6. Brahmachari, G. (2004) Neem-an omnipotent plant: a retrospection. *Chembiochem: a European journal of chemical biology*, **5(4)**, 408–421.

7. Kong, M., Chen, X. G., Xing, K., Park, H. J. (2010) Antimicrobial properties of chitosan and mode of action: A state of the art review. *Int. J. Food Microbio.*, **144**, 51–63. doi: 10.1016/j.ijfoodmicro.2010.09.012.

8. Campos, E. V. R., de Oliveira, J. L., Fraceto, L. F., Singh, B. (2015) Polysaccharides as safer release systems for agrochemicals. *Agron. Sustain. Dev.*, **35**, 47–66. doi: 10.1007/s13593-014-0263-0.

9. Hernández-Téllez, C. N., Plascencia-Jatomea, M., Cortez-Rocha, M. O. (2016) Chitosan in the Preservation of Agricultural Commodities. *Elsevier; Cambridge, MA, USA: Chitosan-based bionano-composites: Development and perspectives in food and agricultural application*s, 315–338.

10. Kashyap, P. L., Xiang X., Heiden P. (2015) Chitosan nanoparticle based delivery systems for sustainable agriculture. *Int. J. Biol. Macromol.*, **77**, 36–51. doi: 10.1016/j.ijbiomac.2015.02.039.

11. Maluin, F. N. & Hussein, M. Z. (2020) Chitosan-Based Agronanochemicals as a Sustainable Alternative in Crop Protection. *Molecules (Basel, Switzerland)*, **25(7)**, 1611. https://doi.org/10.3390/molecules25071611.

12. Hismath, I., Wan Aida, W. M., Ho, C. W. (2011)

Optimization of extraction conditions for phenolic compounds from neem (*Azadirachta indica*) leaves. *International Food Research Journal*, **18(3)**, 931–939.

13. Hoang, N. H., Le Thanh, T., Sangpueak, R., Treekoon, J., Saengchan, C., Thepbandit, W., Papathoti, N. K., Kamkaew, A., Buensanteai, N. (2020) Chitosan Nanoparticles-Based Ionic Gelation Method: A Promising Candidate for Plant Disease Management. *Polymers (Basel)*, **14(4)**, 662. doi:10.3390/polym14040662.

14. Clayton, K. N., Salameh, J. W., Wereley, S. T., Kinzer-Ursem, T. L. (2016) Physical characterization of nanoparticle size and surface modification using particle scattering diffusometry. *Biomicrofluidics*, **10**, 054107. doi:10.1063/1.4962992.

15. Shetta, A., Kegere, J., Mamdouh, W. (2019) Comparative study of encapsulated peppermint and green tea essential oils in chitosan nanoparticles: Encapsulation, thermal stability, in-vitro release, antioxidant and antibacterial activities. *Int. J. Biol. Macromol.*, **126**, 731–742.

16. Nur Ayshah Rosli, German A. Islan, Rosnani Hasham, Guillermo R. Castro, Azila Abdul Aziz (2022) Incorporation of Nanoparticles Based on Zingiber Officinale Essential Oil into Alginate Films for Sustained Release. *Journal of Physical Science*, **33(2)**, 107–124.

17. Mohd Azizi Che Yunus, Ching Yaw Lee, Z. I. (2011) Effects of Variables on The Production of Red-Fleshed Pitaya Powder Using Response Surface Methodology. *Jurnal Teknologi*, **56**, 15–29.

18. Zhu, L. -Y., Yan, X. -Q., Zhang, H. -M., Yao, S. -J., Jiang, L. (2015) Novel double-walled microspheres based on chitosan, sodium cellulose sulfate and sodium tripolyphosphate: Preparation, characterization and in vitro release study. *Korean J. Chem. Eng.*, **32**, 369–372.

19. Lethika D. Nair, Santosh K. Sar, Arun Arora, Deepak Mahapatra (2013) Fourier Transform Infrared Spectroscopy Analysis of Few Medicinal Plants of Chhattisgarh, India. *Journal of Advanced Pharmacy Education & Research*, **3(1)**, 196-200.

20. Keawchaoon, L., Yoksan, R. (2011) Preparation, characterization and in vitro release study of carvacrol-loaded chitosan nanoparticles. *Colloids Surfaces B Biointerfaces*, **84**, 163–171.